



Biological activities of biogenically synthesized fluorescent silver nanoparticles using *Acanthospermum hispidum* leaves extract

Suresh Ghotekar¹ · Shreyas Pansambal² · Sharad P. Pawar^{3,4} · Trupti Pagar⁵ · Rajeshwari Oza² · Sachin Bangale⁶

© Springer Nature Switzerland AG 2019

Abstract

Silver nanoparticles (AgNPs) synthesized by an implicitly environmentally gracious route using *Acanthospermum hispidum* aqueous leaves extract at room temperature reported. This approach is facile, swift, cost-effective and stable for a long time, reproducible at room temperature and in an eco-friendly manner to obtain a self-assembly of AgNPs. These fabricated AgNPs were investigated by ultraviolet–visible spectroscopy, field emission scanning electron microscopy, energy-dispersive X-ray spectroscopy, transmission electron microscope with selected area electron diffraction, X-ray diffraction, Fourier transform Infrared spectroscopy, particle size, zeta potential, photoluminescence with fluorescence life-time spectroscopy and surface area with porosity studies of synthesized nanoparticles were analyzed by Brunauer–Emmett–Teller and Barrett–Joyner–Halenda curve. Besides, these AgNPs displayed antibacterial, antifungal antimycobacterial and antimalarial activity against some bacterial pathogens. From the outcomes obtained it is suggested that AgNPs could be used effectively in future nanobiotechnology and medical concerns.

Keywords Green chemistry · AgNPs · Phytochemicals · Biological activities · Nanotechnology

1 Introduction

Proliferation of nanotechnology has grabbed attention from all fields of science and technology due to the significant and innumerable applications of nanoparticles. Nowadays, the outstanding application of nanomaterials in nanocomputers, nanofertilizers, energy science, cosmetics, food technology, space industry, mechanics, electronic and optical displays, sensors, catalysis and biomedical devices is being explored [1–10]. Over the past some decades, fabrication of several metal nanoparticles such as antimony, copper, gold, palladium, selenium, platinum and silver using fungi, bacteria, and plant extracts is already reported in literature [11–14]. Amongst them

silver has been used as coinage metal and many traditional medicines of Ayurveda in ancient time. Therewithal, AgNPs has attracted considerable attention owing to their various fabulous properties like photocatalysis [15], sensors [16], catalysis [17], antibacterial [18], antiangiogenesis [19], antiviral [20], anti-inflammatory [21], antiseptic sprays, fabrics, topical creams, wound dressing and successfully implemented in the cancer diagnosis and treatment [4, 22, 23].

Heretofore, several notable synthetic routes were employed for the fabrication of AgNPs in the past, such as including laser ablation technique [24], thermal decomposition [25], radiation assisted [26], microwave assisted [27], electrochemical [28] and chemical reduction method [29]. Nevertheless, these conventional chemical and physical

✉ Suresh Ghotekar, ghotekarsuresh7@gmail.com | ¹Department of Chemistry, Sanjivani Arts, Commerce and Science College, Savitribai Phule Pune University, Kopargaon, Maharashtra 423603, India. ²Department of Chemistry, S.N. Arts, D.J.M. Commerce and B.N.S. Science College, Savitribai Phule Pune University, Sangamner, Maharashtra 422605, India. ³Department of Chemistry, Savitribai Phule Pune University, Ganeshkhind, Pune, Maharashtra 411007, India. ⁴PFIC, Grasim Industries, Aditya Birla Group, Taloja MIDC, Navi Mumbai, Maharashtra 410208, India. ⁵Department of Chemistry, G.M.D Arts, B.W Commerce and Science College, Savitribai Phule Pune University, Sinnar, Maharashtra 422103, India. ⁶Department of Chemistry, GMV Science College, University of Mumbai, Tala, Maharashtra 402111, India.



routes are not only energy spendthrift, but also costly and environmentally unfriendly, due to the use of mephitic and perilous chemical [3, 4]. Compared with the conventional routes based on plants or microorganisms have been exhibited in recent years to be cost-effective, swift synthesis, lack of venomous chemicals and environmentally benign and yet produces highly vigorous and stable nanoparticles [3, 4]. Therefore, the biogenic synthesis of nanoparticles represents a linkage among nanotechnology and biotechnology, has gained increasing consideration due to the growing need to develop environmentally benign methodologies for nanomaterial syntheses. Also, biosynthetic method using plant extracts has received more significant attention than chemical and physical methods and even than the utilization of microbes. The method is ideal for nanomaterial fabrication due to the absence of any necessity to maintain an aseptic environment [30]. These developing impetuses of green chemistry, considerable endeavor have been directed toward the biosynthesis of inorganic nanoparticles. Since ancient times, both primary and secondary metabolites of plants (phytochemicals) have demonstrated their importance in Ayurveda, however the use of phytochemicals for the synthesis of metal nanoparticles still remains unexplored and is an area of great research potential. The scrutiny of the literature revealed some notable plant extract used for facile synthesis of AgNPs. For example, *Nervalia zeylanica* [31], *Beutia monosperma* [32], *Leucaena leucocephala* L. [18], *Ipomoea digitata* [33], *Caesalpinia pulcherrima* [34], *Buddleja globosa* [35], *Sacha inchi* [36], *Peganum harmala* [37], unripe fruit of *Annona reticulata* [38], *Ziziphora tenuior* [39], *Caralluma fimbriata* [40], root of *Acanthospermum hispidum* [41], *Pistacia atlantica* [42] and *Rosa Chinensis* L. [43] has been already reported.

Acanthospermum hispidum (AH) belongs family *Asteraceae* is an annual plant (Fig. 1) which is native to tropical America. This plant is also used for many medicinal purposes. Amongst them, leaves and flowering tops of the plant have antimicrobial activity, crushed herb is used in the form of the paste to treat the skin ailments and leaf juice is used to relieve the fever. A scrutiny of the literature revealed some notable pharmacological activities of the drug like antimicrobial, anthelmintic, antiviral, antiplasmodial, antitumor, antibacterial and antidiarrheal activity [44–50]. In the present study, AgNPs have been easily and rapidly fabricated using leaves extract of AH. Biological activities of these nanoparticles were evaluated using disc diffusion method, Lowenstein–Jensen (L. J.) method and JSB stain method.



Fig. 1 Leaves of *Acanthospermum hispidum* L. plant

2 Materials and methods

2.1 Materials

AH fresh leaves were sourced from Chandwad college campus, Nashik, Maharashtra, India. The collected leaves were cleaned with deionized water and chopped into small pieces. Silver nitrate (AgNO_3 , 99.99%, analytical grade, Sigma-Aldrich), sodium bicarbonate (NaHCO_3 , analytical grade, 99.7%, Sigma-Aldrich), dimethyl sulfoxide (DMSO, ACS reagent, 99.9%, Sigma-Aldrich) and deionized water were used as raw materials without additional purification. All glassware used in the laboratory experiments was cleaned with a solution of acetone, washed thoroughly with deionized water, and dried in oven before use.

2.2 Biogenic synthesis of AgNPs

10 g small wized pieces of AH leaves were transferred into 250 mL beaker containing 100 mL deionized water. The mixture were refluxed at 80–90 °C for 20 min and cooled at room temperature followed by filtered through ordinary filter paper. Then, resultant filtrate was again filtered through Whatmann No. 1. The filtered extract is stored in refrigerator at 4 °C and used for synthesis of AgNPs. The aqueous solution of 1 mM AgNO_3 was prepared in deionized water. AH leaf extract was added to 1 mM aqueous AgNO_3 solution in 1:1 ratios in a 250 mL beaker with constant stirring on magnetic stirrer at

500 rpm for 25 min. After time of period the color of solution turns to dark brown. The resultant solution was centrifuged at room temperature by using cooling centrifuge machine at 15,000 rpm and the residue was collected after discarding the supernatant liquid. The collected AgNPs were allowed to dry in a petri dish. The schematic representation of biogenic synthesis of AgNPs is shown in Fig. 2. A black colored powder was obtained and this was carefully collected and packed for characterization purposes.

2.3 Characterization techniques

The morphology and composition of the rapidly fabricated AgNPs were examined by field emission scanning electron microscopy (FE-SEM) and energy-dispersive X-ray spectroscopy (EDX) using Nova Nano SEM 450 and Bruker, XFlash 6130 respectively. Find the exact morphological structures and size of the AgNPs using transmission electron microscopic (TEM) analysis is done by using a PHILIPS CM200. The crystallinity, crystal plane and phases were characterized by X-ray diffraction (XRD, Bruker, D8-Advanced Diffractometer) pattern measured with Cu-K α Radiation ($\lambda = 1.5406 \text{ \AA}$) in the range of 20° – 80° . The Fourier transform Infrared (FTIR) spectrum was recorded in the range of 4000 – 400 cm^{-1} by using JASCO 4100. The particle size distribution and surface charge of AgNPs were determined using particle size analyzer (Malvern Instruments Ltd., Zetasizer Ver. 6.34) at 25° C with 90° detection angle. Photoluminescence nature of biogenically synthesized AgNPs was evaluated by using JOBIN–YVON FLUROLOG-3-11 Spectrofluorimeter. The N_2 absorption–desorption isotherms, specific surface area and porosity were characterized by Brunauer–Emmett–Teller (BET) and Barrett–Joyner–Halenda (BJH) analysis method at 77.40° K (NOVA-100 Ver. 3.70)



Fig. 2 Schematic presentation for the green synthesis of AgNPs

2.4 Phytochemical screening

The fresh aqueous leaves extract of AH were investigated for the presence of phytochemicals viz. coumarins, saponins, tannin, flavonoids, volatile oils, sterols and phenols by standard biochemical protocols [51]. The chemical tests were performed by reported methods.

2.4.1 Test for tannins

2 mL leaves extract of AH was added to few drops of 10% FeCl_3 which gives yellowish precipitate, shows presence of tannin in the plant extract.

2.4.2 Test for saponins

5 mL leaves extract was mixed with 20 mL water and then agitated into graduated cylinder for 15 min formation of foam. This indicates presence of saponins.

2.4.3 Test for flavonoids

3 mL of 1% NH_4Cl solution was added to 5 ml of leaves extract, which gives yellow color, i.e. presence of flavonoids.

2.4.4 Test for phenols

5% ferric chloride was added to the 2 mL leaves extract which shows black colouration. This indicates presence of phenols.

2.4.5 Test for steroids

1 mL leaves extract dissolved in 10 mL chloroform and equal volume of concentrated H_2SO_4 was added by sides of the test tube. The upper layer turns red and H_2SO_4 layered showed yellow with green fluorescence. This indicates steroids are present.

2.4.6 Test for coumarins

Conc. HCl and a few drop of Ehrlich reagent was mixed with 2 mL plant extract, which gives appearance of yellow color. This shows presence of coumarins.

2.4.7 Test for glycosides

2 mL leaves extract was mixed with 3 mL of chloroform and 1 ml 10% NH_3 solution was added. There is no

change in the color of plant extract. This indicates glycosides are absent.

2.4.8 Test for proteins

The leaves extract was heated with distilled water and filtered. To this filtrate 2% CuSO₄, 95% ethanol and KOH was added. There is no formation of a pink ethanolic layer. This indicates the proteins are absent.

2.4.9 Test for anthraquinone

A few drops of magnesium acetate solution were mixed with leaves extract. There is no formation of pink color. This indicates anthraquinone are absent.

2.5 Antibacterial activity of synthesized AgNPs

The antibacterial assay of biogenically synthesized AgNPs was examined by using disk diffusion method. This method was employed against human pathogenic (*Pseudomonas aeruginosa* MTCC-1688, *Streptococcus pyogenes* MTCC-442, *Staphylococcus aureus* MTCC-96, *Escherichia coli* MTCC-443) bacteria grown in nutrient Agar medium at 37 °C for 24 h. The nutrient agar medium plates were prepared, well sterilized and solidified. After solidification, bacterial cultures spread over the plate. Sterile Whatmann filter paper disks were loaded with different concentrations of synthesized AgNPs and control in each plate. These plates were incubated in incubator at 37 °C for 24 h and diameter of inhibition zones were measured against bacterial strain and standard drug [18].

2.6 In vitro antifungal activity of synthesized AgNPs

Antifungal activity of synthesized AgNPs examine against fungal strains (*Candida albicans* MTCC 227, *Aspergillus niger* MTCC 282 and *Aspergillus clavatus* MTCC 1323) using the agar dilution method [52]. Determine the minimum inhibitory concentration (MIC), a stock solution of the biosynthesized AgNPs was prepared in dimethyl sulfoxide and then were incorporated in a molten sterile agar, i.e., dextrose agar for antifungal screening. The inoculums were prepared by taking a stock culture to about 100 mL of nutrient broth, in 250 mL clean and sterilized conical flasks. The flasks were incubated at 27 °C for 24 h before use. The plates were kept in aseptic condition at room temperature to allow diffusion of the solution properly into potato-dextrose-agar medium. Then the culture plates were incubated at 25 °C for 48 h. The highest dilution showing at least 99% inhibition zone is taken as MIC and Greseofulvin were used as a reference drug for the

experiment of antifungal activity. The experiments were performed in triplicate in order to minimize the errors of whole method.

2.7 In vitro antimycobacterial screening of synthesized AgNPs

The antimycobacterial activity of biogenically synthesized AgNPs was obtained for *Mycobacterium tuberculosis* H₃₇RV, by using L. J. MIC protocol [53]. Stock solutions of AgNPs (various concentrations) in DMSO were added in the liquid L. J. Medium and after that media were sterilized. The *Mycobacterium tuberculosis* H₃₇RV culture was growing on L. J. medium and harvested in bijou bottles (0.85% saline). These tubes were then incubated at 37 °C for 24 h followed by streaking of *Mycobacterium tuberculosis* H₃₇RV. These tubes were then incubated at 37 °C. Development of bacilli was seen after 12 days, 22 days and finally 28 days of incubation respectively. Tubes having the AgNPs were compared with control tubes where medium alone was incubated with *M. tuberculosis* H₃₇RV. The concentration at which no growth of colonies occurred or < 20 colonies was taken as MIC concentration of test compound. The standard strain *M. tuberculosis* H₃₇RV was tested with known drug isoniazid.

2.8 In vitro antimalarial screening of synthesized AgNPs

The in vitro antimalarial assay was carried out in 96 well microtitre plates according to the protocol of antimalarial activity [54]. The cultures of *Plasmodium falciparum* strain were maintained in RPMI-1640 supplemented medium with 25 mM HEPES, 0.23% NaHCO₃, 1% D-glucose and 10% heat inactivated human serum. The *Plasmodium falciparum* were synchronized after 5% D-sorbitol treatment to get only the ring stage parasitized cells. For carrying out the assay, an initial ring stage parasitaemia of 3% haematocrit in a total volume of 200 µl of medium RPMI-1640 was determined by Jaswant Singh Bhattacharya (JSB) staining [55] to evaluate the percent parasitaemia and uniformly maintained with 50% RBCs. The plates were incubated at 37 °C, after 36 h incubation, thin blood smears from every well were prepared and stained with JSB stain. Thereafter, slides were microscopically observed to note that maturation of the ring stage parasites into schizonts and trophozoites in the presence of various concentrations of the biosynthesized AgNPs. Therein, biosynthesized AgNPs concentration which inhibited the complete maturation into schizonts was recorded as the MIC. Chloroquine and Quinine were used as the standard reference drugs for experiments [18].

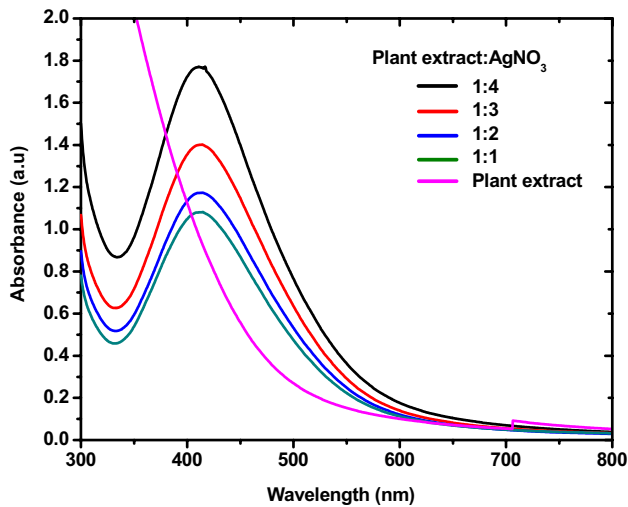


Fig. 3 UV-Vis spectra for the biogenic synthesis of AgNPs using aqueous leaves extract of *Acanthospermum hispidum*

3 Results and discussion

3.1 UV-visible spectral studies

To study the stability and formation of AgNPs was ascertained by surface plasmon resonance band (SPR) using UV-Vis spectroscopy. Figure 3 shows the visual calorimetric pattern of samples after the reaction at different concentrations of plant extract and AgNPs. The colorless AgNO_3 solution turned yellow to brown indicated the formation of AgNPs. It is observed that, there is an appearance of absorbance peak around 417 nm and usually spherical AgNPs having λ_{max} values were reported earlier in the visible range of 400–475 nm.

3.2 Structural and crystallographic analysis

The standard conditions stable phase of AgNPs is a cubic phase within the space group $\text{Fm}\bar{3}\text{m}$. Figure 4 reports a typical XRD profile of the synthesized AgNPs. Powder XRD of biogenically fabricated AgNPs was done using monochromatic $\text{CuK}\alpha\text{-1}$ radiation (wavelength 1.5406 Å), operating at a current of 40 mA and voltage of 40 kV, in the precise range 2θ of $20^\circ\text{--}80^\circ$. Four prominent Bragg peaks were observed at $2\theta = 38.10^\circ, 44.40^\circ, 64.50^\circ$ and 77.50° which corresponds to (111), (200), (220) and (311) Bragg's reflections of the face-centered cubic (FCC) structure of metallic silver, respectively. The XRD profile data of AgNPs is in good assent with the standard JCPDS file no. 04-0783 and the nanoparticles size of the AgNPs formed were calculated using Debye-Scherrer's equation [56] which was around 25–45 nm, were good in concurrence with FE-SEM results also. Overall optostructural study signifies

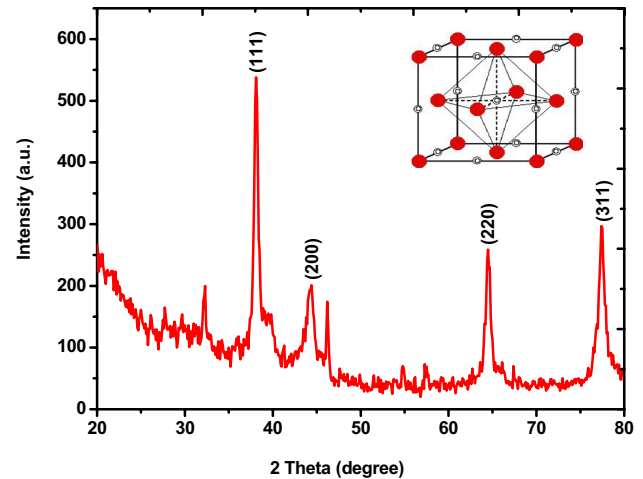


Fig. 4 X-ray diffraction profile of biogenically synthesized AgNPs at room temperature

that fabricated material has pure FCC crystal nanostructure with polycrystalline nature.

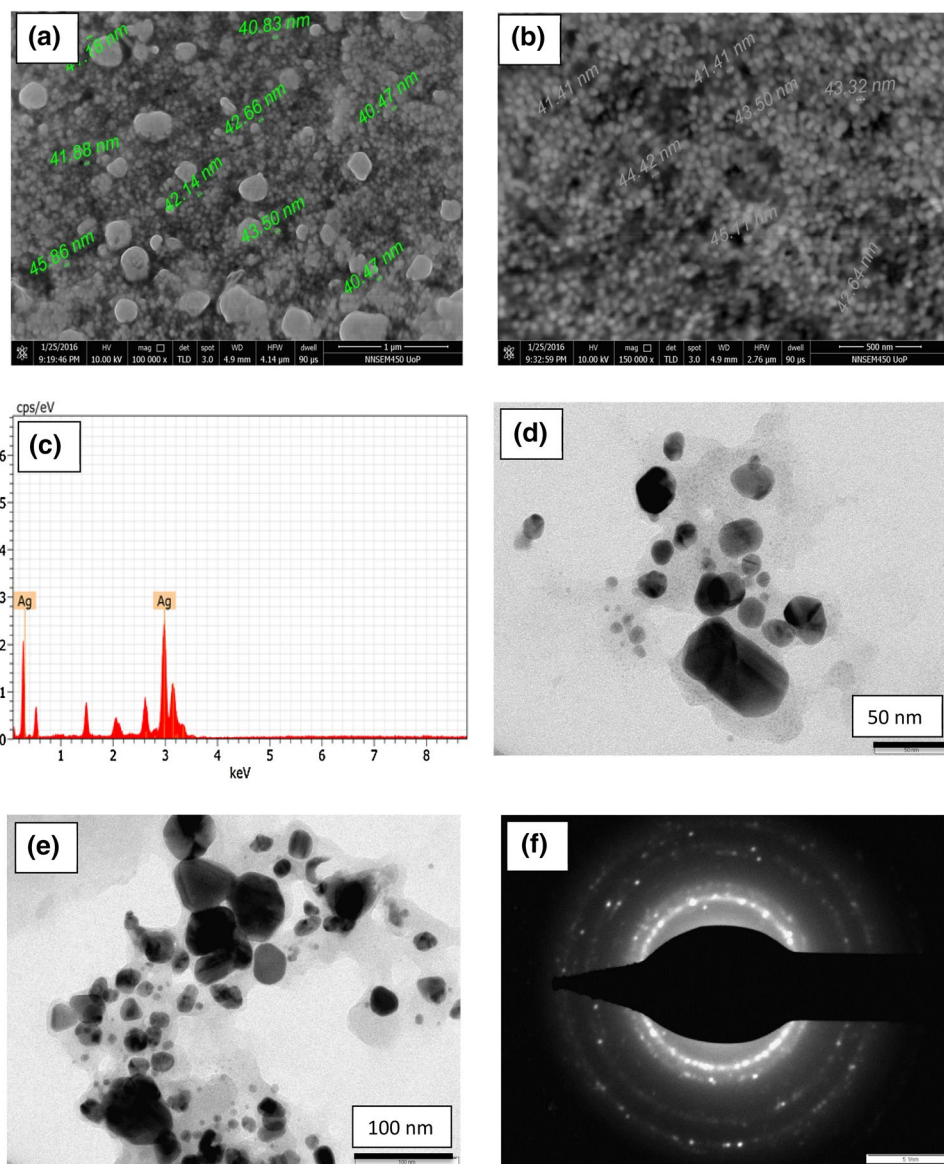
3.3 Morphological studies and elemental analysis

The morphology of biosynthesized AgNPs is viewed by FE-SEM microphotographs. Figure 5a, b show a well monodispersed AgNPs have identified in the sizes range of 40–46 nm and there are not in direct contact even within the aggregates indicating stabilization of nanoparticles by capping agents. The strong signal of silver in EDX spectrum affirms the formation of biogenic synthesis of AgNPs. Metallic silver nanocrystals generally evince (Fig. 5c) typical optical absorption peak approximately at 3 keV because of surface plasmon resonance [57]. Elemental composition of silver confirms the complete reduction of silver ions to AgNPs as shown in the spectrum. The TEM images provided additional insight into the morphological shape and size details of the biogenically fabricated AgNPs. The TEM images at different magnifications and SAED patterns are depicted in the Fig. 5d, e. The quasi-spherical nature of the AgNPs was also witnessed by the TEM with average diameter ranging 20–60 nm. The results ascribed from the XRD studies are in good agreement with SAED pattern which suggests the polycrystalline nature of AgNPs (Fig. 5f).

3.4 Particle size distribution and zeta potential measurement

The results of DLS analysis exhibit the average size of nanoparticles is 32 nm (Fig. 6a). Zeta potential is an extensive parameter for understanding the state of the nanoparticle surface and predicting the long-term stability of the

Fig. 5 **a, b** FE-SEM observation of biogenically synthesized AgNPs, **b** energy dispersive X-ray (EDX) spectrum showed higher percentage of silver signals, **c** TEM image of AgNPs at 50 nm range and, **d** 100 nm range and, **f** SAED patterns of the AgNPs exhibit concentric rings, indicating that these nanoparticles are highly crystalline in nature



dispersion. The negative potential value supports long high degrees of term stability, good colloidal nature and high dispersity of AgNPs due to negative–negative repulsion. Dispersions with a low zeta potential value will inevitably aggregate due to inter particle attractions. Figure 6b shows the zeta potential value of dispersed biogenically synthesized AgNPs in deionized water without any electrolyte was -6.23 mV, and formed neutral charge on bio-synthesized AgNPs (Ag^0).

3.5 Vibrational properties

FTIR analysis was used to determine the functional groups present in the Fig. 7. The broad band seen at 3786 cm^{-1} reveals the presence of an $-\text{OH}$ group,

resulting from either alcoholic or phenolic stretching, while the peaks around 2964 cm^{-1} are attribute to frequency of the C–H bond (asymmetric stretching vibration) in alkanes. The peaks observed at 1706 corresponds to C=O (carbonyl group) stretching frequency of conjugated cyclic ketones. The peaks around 1601 cm^{-1} may be attributed to C=C in aromatic compounds. The strong peak observed at 1016 cm^{-1} corresponds to C–O stretching frequency of ester in the aqueous leaves extract of AH. The FTIR results confirm the presence of phytochemicals in the plant extract such as, which further act as reducing/capping agents for the fabrication of AgNPs and is in good agreement with the phytochemical profile of aqueous leaves extract of AH.

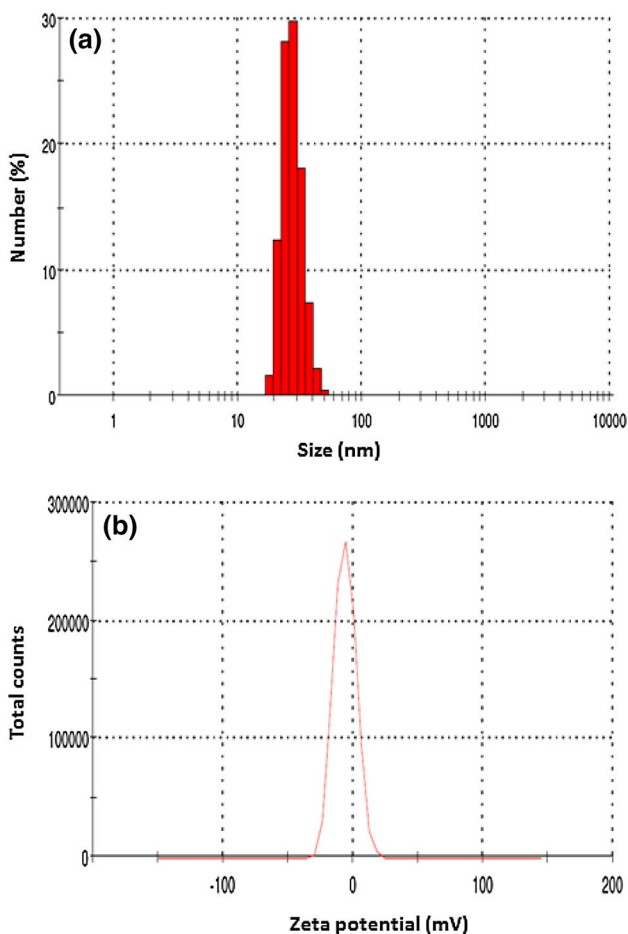


Fig. 6 **a** Zeta sizer and **b** zeta potential of biogenically synthesized AgNPs

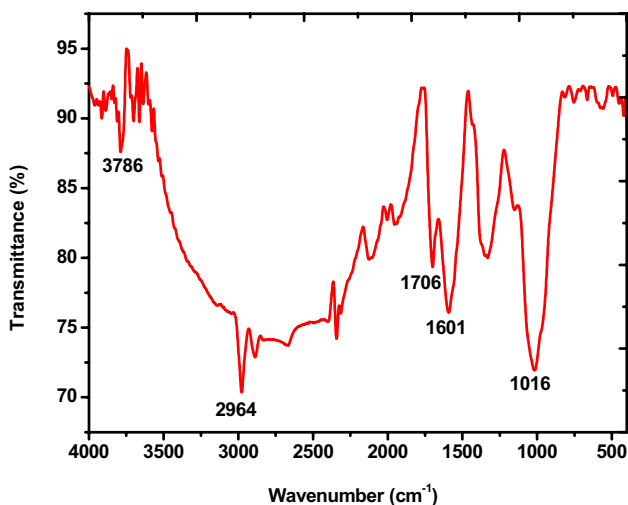


Fig. 7 FT-IR spectrum of biogenically synthesized AgNPs

3.6 Specific surface area and porosity studies

The shape, density and particle size of nanomaterial are main parameters related to the specific surface area (SSA) measurements (m^2/g). The SSA of AgNPs computed using the multipoint BET-equation is $9.91 m^2/g$. Assuming that the particles have solid, spherical shape with smooth surface and the surface area can be related to the average equivalent particle size by the equation,

$$D_{BET} = 6000 / (\rho \cdot Sw) \quad (\text{in nm})$$

where, D_{BET} is the average diameter of a spherical particle, ρ is the theoretical density in g/cm^3 and Sw represents the specific surface area of the powder in m^2/g . The average crystallite size of the AgNPs is $57.66 nm$ and which is ascertained from BET data utilizing above equation. We noticed that the particle size obtained from the BET and the FESEM methods concurs very well with the result given by X-ray line broadening. The results of TEM observations and BET techniques additionally confirmed and verified the relevant results obtained by XRD as mentioned above. Figure 8 demonstrates the typical BJH desorption pore size distribution curves of AgNPs. From the curves, most of the micropores with a size smaller than $29.63 nm$, the pore size of which estimated from the peak position are about $3.16 nm$ and pore volume is $0.0078 cc/g$. Therefore, these synthesized particles are actually grain clusters and nanocrystalline in nature.

The N_2 absorption–desorption isotherms of the AgNPs were examined by using the static volumetric absorption analyzer. Figure 9 demonstrates the typical nitrogen sorption isotherms of AgNPs. It demonstrates the sample presents typical adsorption, in the low-pressure region ($P/P_0 < 0.3$). Graph shows that the isotherms relative flat, the adsorption and desorption isotherms totally superposition

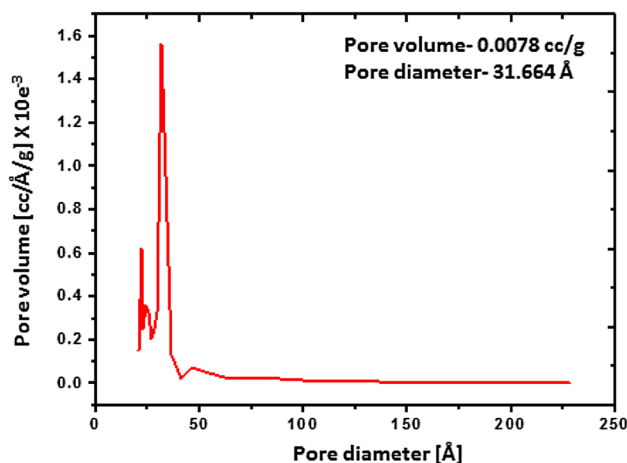


Fig. 8 BJH pore size distribution curves plots of biosynthesized AgNPs

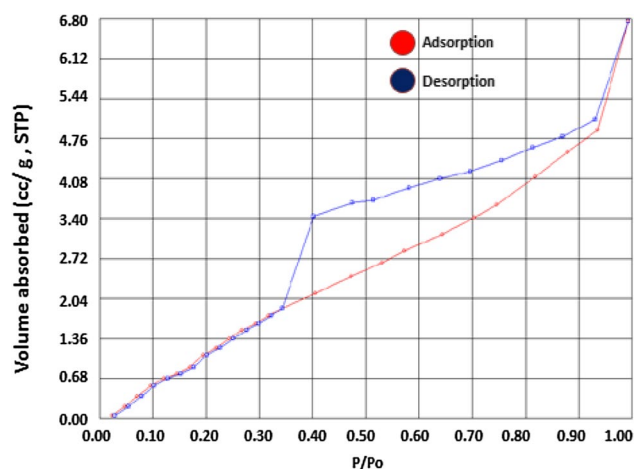


Fig. 9 N_2 adsorption–desorption isotherm of biosynthesized AgNPs

Table 1 Phytochemical profile of aqueous leaves extract of *Acanthospermum hispidum*

Phytoconstituents	Test	Phytoconstituents	Test
Tannin	+	Saponins	+
Coumarins	+	Emodins	–
Proteins	–	Flavonoid	+
Glycosides	–	Anthraquinone	–
Anthocyanin	–	Sterols	+
Phenols	+	Volatile oils	+

and generally adsorption of the samples mostly occurs in the micropores. At the relative high pressure region ($P/P_0 > 0.3$), due to the capillary agglomeration phenomenon, the isotherms increase very quickly and form a lag loop.

3.7 Phytochemical screening

The results of qualitative pharmacognostic assess of aqueous leaf extract of AH are shown in Table 1. Phytochemical profile of AH leaves [57] revealed and highlighted the presence of saponins, coumarins, phenols, flavonoids, volatile oils, tannins and sterols which may be accountable for the efficient capping and chelating agent of nanoparticles and this was further confirmed by FTIR spectrum [57]. The physical and chemical processes driving the reaction of the natural extract of the AH and the silver nitrate precursor and the reaction dynamic will be investigated through adequate characterization techniques in perspective of identifying the development of the AgNPs. Figure 10

highlighted the bioactive chemical compounds from the natural extract of AH [58].

3.8 Photoluminescence study

AgNPs are reported to exhibit visible photoluminescence and their fluorescence spectra are appeared in Fig. 11. The optimized AgNPs were found to be luminescent with two emissions at 436 and 674 nm for an excitation at 390 nm. The luminescence at 390 nm may be because of presence of phytoconstituents or antioxidants present in the plant extract [57].

3.9 Fluorescence life-time studies

The chemical information of nanomaterial can often be gained from the time-dependent nature of fluorescence. Time-resolved fluorescence provides more information about the molecular environment of the fluorescent compound than steady state fluorescence measurements [59]. It is important to remember that the fluorescence lifetime is an average time for a molecule to remain in the excited state before emitting a photon. Every individual molecule emits randomly after excitation. Many excited molecules will fluorescent before the average lifetime; however some will also fluorescent long after the average lifetime. Fluorescence lifetimes are normally on the time scale order of nanosecond (ns) to the sub-nanosecond.

Figure 12a, b shows fluorescence decay profile for AgNPs. The fluorescence lifetime of biogenically fabricated AgNPs were fitted in multi-exponential decay curves. The average fluorescence lifetimes of AgNPs are 2.9028 ns (emission at 674 nm) and 1.8572 ns (emission at 436 nm) respectively. The data shows that greater fluorescence lifetime when emission at 674 nm than emission at 436 nm. It is known that aggregation and molecular interactions lead to a prolonged lifetime [57, 59, 60]. The long lifetimes at 674 nm compared with that of a 436 nm are attributed to the formation of aggregated nanoparticles that restricts the molecular rotation and vibration of molecules and thus increases the emission lifetime at 674 nm. However, fluorescence lifetime of AgNPs at 674 nm is greater than at 436 nm.

3.10 Antibacterial activity of AgNPs

The antibacterial activities of biosynthesized AgNPs were investigated against pathogenic bacteria using disk diffusion method and exact zone of inhibition was measured

Fig. 10 Major bioactive compounds in the natural extract of *Acanthospermum hispidum*

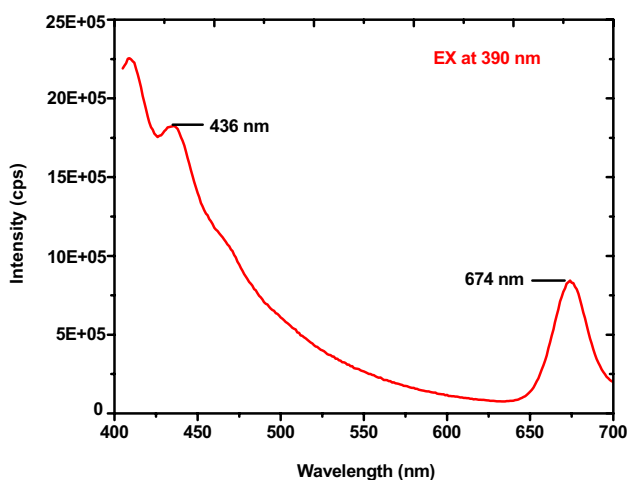
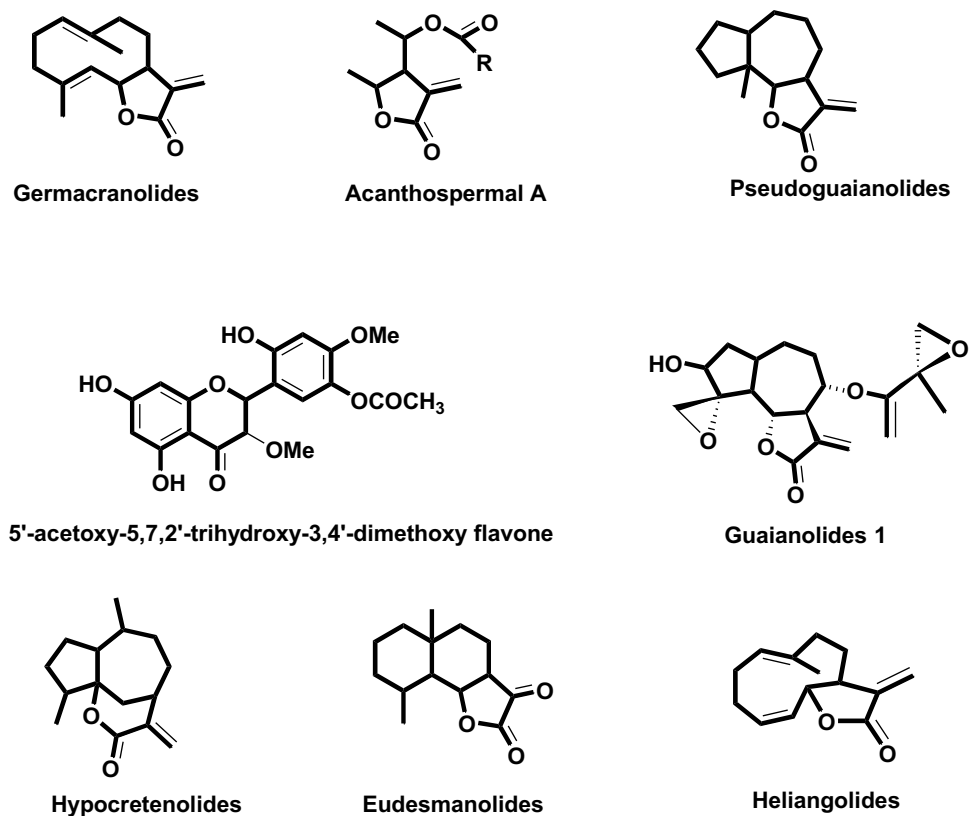


Fig. 11 Fluorescence spectra of biogenically synthesized AgNPs formed with excitation at 390 nm

with respect to positive controls (Table 2). In present study, zone of inhibition was found to be highest (23 mm) against *S. pyogenus* and lowest (12 mm) against *E. coli*. These outcomes are in agreement with preceding studies that examined antibacterial activity of AgNPs [18].

3.11 Antifungal activity of AgNPs

The results of antifungal activity of the biosynthesized AgNPs are presented in Table 3. The antifungal activity of the synthesized AgNPs was determined in vitro using an Agar plate method against selected strains viz. *C. albicans*, *A. niger* and *A. clavatus* at different concentration ranging between 100 µg/ml to 1250 µg/ml. Fabricated AgNPs exhibited a moderate activity against *C. albicans* at concentration of 500 µg/ml reference standard Griseofulvin at concentration 500 µg/mL.

3.12 Antimycobacterial activity of AgNPs

The antimycobacterial screening was accomplished using L-J MIC protocol (Table 4) and it is worthwhile to observe that biosynthesized AgNPs was the only displaying inhibition of *Micobacterium tuberculosis* H₃₇RV totally (99%) at the MIC of 100 µg/ml.

3.13 Antimalarial activity of biosynthesized AgNPs

The biosynthesized AgNPs were screened for their in vitro antimalarial activity against *Plasmodium falciparum* by

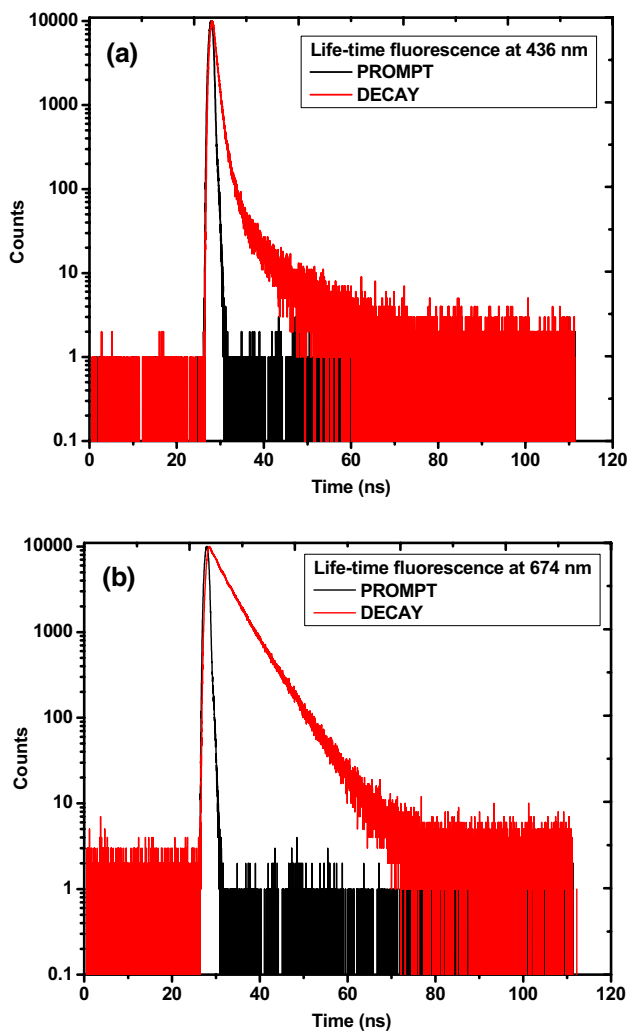


Fig. 12 Fluorescence life-time spectra of biogenically synthesized AgNPs at **a** 436 nm and **b** 674 nm

measuring the MIC ($\mu\text{g}/\text{mL}$) against standard reference drugs like Quinine and Chloroquine, as shown in Table 5.

Table 2 Zone of inhibition (mm) of biosynthesized AgNPs against bacterial pathogens

Test pathogens	Inhibition zone (mm) of AgNPs ($\mu\text{g}/\text{ml}$)					Ampliciline ($\mu\text{g}/\text{ml}$)
	25	50	100	250	500	
<i>E. coli</i>	12	15	17	18	22	19
<i>P. aeruginosa</i>	14	16	17	18	20	18
<i>S. pyogenus</i>	13	17	19	20	23	18
<i>S. aureus</i>	13	15	17	19	21	16

Table 3 MIC of AgNPs against fungal pathogens

Test pathogens	MIC ($\mu\text{g}/\text{ml}$) of AgNPs	MIC ($\mu\text{g}/\text{ml}$) of griseofulvin
<i>C. albicans</i> (MTCC 227)	500	500
<i>A. niger</i> (MTCC 282)	250	100
<i>A. clavatus</i> (MTCC 1323)	500	100

Table 4 MIC of biosynthesized AgNPs against *Mycobacterium tuberculosis*

S. no.	Compound name	MIC ($\mu\text{g}/\text{ml}$)
1.	AgNPs	100
2.	Isoniazid (standard)	0.20

Table 5 MIC of biosynthesized AgNPs against *Plasmodium falciparum*

S. no.	Compound name	Mean IC_{50} values ($\mu\text{g}/\text{ml}$)
1.	AgNPs	0.91
2.	Chloroquine (standard)	0.020
3.	Quinine (standard)	0.268

4 Conclusion

The present study demonstrates the utilization of unreported aqueous extracts of AH for the reliable and quick synthesis of AgNPs from silver nitrate. Variation in reaction conditions influenced nanoparticle fabrication where the reaction mixtures evinced typical colors and UV-visible spectra, characteristic of AgNPs. The biosynthesized nanoparticles produced by this cost-effective, non-toxic, swift and environmentally benevolent protocol were

characterized by a variety of standard analytical techniques like XRD, SEM, and TEM and were further tested against bacterial pathogens. Besides, this protocol could be easily scaled up for the modern industrial applications to increase the yield of the nanoparticles significantly, which undoubtedly would establish its commercial viability in medicine. Nanoparticle synthesis is a novel research area to search for an eco-friendly manner and green materials for miraculous applications in the fields of nanomedicine and drug delivery.

Acknowledgements We are thankful to CIF Savitribai Phule Pune University, North Maharashtra University, BIT Bengaluru, SAIF IIT Powai, SAIF IIT Madras and Microcare Laboratory Gujrat for providing the technical, instrumental and biological activities supports for this research work. We are also thankful to Ajay Savale and Sahebrao Nagare for his help during experimental work.

Compliance with ethical standards

Conflict of interest The authors declare no conflict of interest in this work.

References

- Daniel MC, Astruc D (2004) Gold nanoparticles: assembly, supramolecular chemistry, quantum-size-related properties, and application toward biology, catalysis, and nanotechnology. *Chem Rev* 104:293–334
- Chaudhari RG, Paria S (2012) Core/shell nanoparticles: classes, properties, synthesis mechanisms, characterization, and applications. *Chem Rev* 112:2373–2433
- Ghotekar S (2019) A review on plant extract mediated biogenic synthesis of CdO nanoparticles and their recent applications. *Asian J Green Chem* 3(2):187–200
- Ahmed S, Ahmad M, Swami BL, Ikram S (2016) A review on plant extract mediated synthesis of silver nanoparticles for antimicrobial applications: a green expertise. *J Adv Res* 7:17–28
- Aher YB, Jain GH, Patil GE, Savale AR, Ghotekar SK, Pore DM, Pansambal SS, Deshmukh KK (2017) Biosynthesis of copper oxide nanoparticles using leaves extract of *Leucaena leucocephala* L. and their promising upshot against the selected human pathogens. *Int J Mol Clin Microbiol* 7(1):776–786
- Frewer LJ, Gupta N, George S, Fischer ARH, Giles EL, Coles D (2014) Consumer attitudes towards nanotechnologies applied to food production. *Trends Food Sci Technol* 40:211–225
- Kamble DR, Bangale SV, Ghotekar SK, Bamane SR (2018) Efficient synthesis of CeVO₄ nanoparticles using combustion route and their antibacterial activity. *J Nanostruct* 8(2):144–151
- Nikam A, Pagar T, Ghotekar S, Pagar K, Pansambal S (2019) A review on plant extract mediated green synthesis of zirconia nanoparticles and their miscellaneous applications. *J Chem Rev* 1(3):154–163
- Ghotekar S, Pansambal S, Pagar K, Pardeshi O, Oza R (2018) Synthesis of CeVO₄ nanoparticles using sol-gel auto combustion method and their antifungal activity. *Nanochem Res* 3(2):189–196
- Savale A, Ghotekar S, Pansambal S, Pardeshi O (2017) Green synthesis of fluorescent CdO nanoparticles using *Leucaena leucocephala* L. extract and their biological activities. *J Bacteriol Mycol Open Access* 5(5):00148
- Bhainsa KC, D'Souza SF (2006) Extracellular biosynthesis of silver nanoparticles using the fungus *Aspergillus fumigates*. *Colloids Surf B* 47:160–164
- Ahmad A, Mukherjee P, Senapati S, Mandal D, Khan MI, Kumar R, Sastry M (2003) Extracellular biosynthesis of silver nanoparticles using the fungus *Fusarium oxysporum*. *Colloids Surf B* 28:313–318
- Shahverdi R, Minaeian S, Shahverdi HR, Jamalifar H, Nohi AA (2007) Rapid synthesis of silver nanoparticles using culture supernatants of enterobacteria: a novel biological approach. *Proc Biochem* 42:919–923
- Senapati S, Ahmad A, Khan MI, Sastry M, Kumar R (2005) Extracellular biosynthesis of bimetallic Au–Ag alloy nanoparticles. *Small* 1:517–520
- Paul B, Bhuyan B, Purkayastha DD, Dhar SS (2015) Green synthesis of silver nanoparticles using dried biomass of *Diplazium esculentum* (retz.) sw. and studies of their photocatalytic and anticoagulative activities. *J Mol Liq* 212:813–817
- Tagad CK, Dugasani SR, Aiyer R, Park S, Kulkarni A, Sabharwal S (2013) Green synthesis of silver nanoparticles and their application for the development of optical fiber based hydrogen peroxide sensor. *Sens Actuators B Chem* 183:144–149
- Bhosale MA, Bhanage BM (2015) Silver nanoparticles: synthesis, characterization and their application as a sustainable catalyst for organic transformations. *Curr Org Chem* 19:1–15
- Ghotekar S, Savale A, Pansambal S (2018) Phytofabrication of fluorescent silver nanoparticles from *Leucaena leucocephala* L. leaves and their biological activities. *J Water Environ Nanotechnol* 3(2):95–105
- Gurunathan S, Lee KJ, Kalishwaralal K, Sheikpranbabu S, Vaidyanathan R, Eom SH (2009) Antiangiogenic properties of silver nanoparticles. *Biomaterials* 30:6341–6350
- Elechiguerra JL, Burt JL, Morones JR, Camacho-Bragado A, Gao X, Lara HH, Yacaman MJ (2005) Interaction of silver nanoparticles with HIV-1. *J Nanobiotechnol* 3:6
- Nadworny PL, Wang J, Tredget EE, Burrell RE (2008) Anti-inflammatory activity of nanocrystalline silver in a porcine contact dermatitis model. *Nanomedicine* 4:241–251
- Kathiravan V, Ravi S, Kumar SA (2014) Synthesis of silver nanoparticles from *Meliadubia* leaf extract and their in vitro anticancer activity. *Spectrochim Acta Part A Mol Biomol Spectrosc* 130:116–121
- Popescu M, Velea A, Lorinczi A (2010) Biogenic production of nanoparticles. *Dig J Nanomater Biostruct* 5:1035–1040
- Mafunè F, Kohno J, Takeda Y, Kondow T, Sawabe H (2000) Formation and size control of silver nanoparticles by laser ablation in aqueous solution. *J Phys Chem B* 104:9111–9117
- Plante IJL, Zeid TW, Yangab P, Mokari T (2010) Synthesis of metal sulfide nanomaterials via thermal decomposition of single-source precursors. *J Mater Chem* 20:6612–6617
- Cheng Y, Yin L, Lin S, Wiesner M, Bernhardt E, Liu J (2011) Toxicity reduction of polymer-stabilized silver nanoparticles by sunlight. *J Phys Chem* 115:4425–4432
- Nadagauda MN, Speth TF, Varma RS (2011) Microwave-assisted green synthesis of silver nanoparticles. *Acc Chem Res* 44:469–478
- Hirsch T, Zharnikov M, Shaporenko A, Stahl J, Wiess D, Wolfbeis OS (2005) Size-controlled electrochemical synthesis of metal nanoparticles on monomolecular templates. *Angew Chem* 44:6775–6778
- Ghotekar SK, Vaidya PS, Pande SN, Pawar SP (2015) Synthesis of silver nanoparticles by using 3-methyl pyrazol 5-one (chemical reduction method) and its characterizations. *Int J Multidiscip Res Dev* 2(5):419–422

30. Rai A, Singh A, Ahmad A, Sastry M (2006) Role of halide ions and temperature on the morphology of biologically synthesized gold nanotriangles. *Langmuir* 22:736–741
31. Vijayan R, Joseph S, Mathew B (2018) Green synthesis of silver nanoparticles using *Nervalia zeylanica* leaf extract and evaluation of their antioxidant, catalytic and antimicrobial potentials. *Part Sci Technol* 37(7):1–11
32. Pattanayak S, Mollick MMR, Maity D, Chakraborty S, Dash SK, Roy S, Chattopadhyay S, Chattopadhyay D, Chakraborty M (2017) *Butea monosperma* bark extract mediated green synthesis of silver nanoparticles: characterization and biological application. *J Saudi Chem Soc* 21:673–684
33. Varadavenkatesan T, Selvaraj R, Vinayagam R (2018) Dye degradation and antibacterial activity of green synthesized nanoparticles using *Ipomoea digitata* Linn. flower extract. *Int J Environ Sci Technol* 3:1–10
34. Moteria P, Chanda S (2017) Synthesis and characterization of silver nanoparticles using *Caesalpinia pulcherrima* flower extract and assessment of their in vitro antimicrobial, antioxidant cytotoxic and genotoxic activities. *Artif Cells Nanomed Biotechnol* 45:1556–1567
35. Carmona ER, Benito N, Plaza T, Recio-Sánchez G (2017) Green synthesis of silver nanoparticles by using leaf extract from the endemic *Buddleja globosa* hope. *Green Chem Lett Rev* 10:250–256
36. Kumar B, Smita K, Cumbal L, Debut A (2017) Sacha inchi (*Plukenetia volubilis* L.) shell biomass for synthesis of silver nanocatalyst. *J Saudi Chem Soc* 21:S293–S298
37. Azizi M, Sedaghat S, Tahvildari K, Derakshi P, Ghaemi A (2017) Synthesis of silver nanoparticles using *Peganum harmala* extract as a green route. *Green Chem Lett Rev* 10:420–427
38. Ghotekar SK, Pande SN, Pansambal SS, Sanap DS, Mahale KM, Sonawane B (2015) Biosynthesis of silver nanoparticles using unripe fruit extract of *Annona reticulata* L. and its characterization. *World J Pharm Pharm Sci* 4(11):1304–1312
39. Sadeghi B, Gholamhoseinpoor F (2015) A study on the stability and green synthesis of silver nanoparticles using *Ziziphora tenuior* (Zt) extract at room temperature. *Spectrochim Acta A Mol Biomol Spectrosc* 134:310–315
40. Pande SN, Bharati KT, Wakchure SK, Ghotekar SK, Gujrathi DB, Phatangare ND (2015) Green synthesis of silver nanoparticles by *Caralluma fimbriata* and its characterization. *Indian J App Res* 5(2):749–750
41. Vani BKK (2014) Biosynthesis and characterization of silver nanoparticles from *Acanthospermum hispidum* root extract. *J Adv Stud Agric Biol Environ Sci* 1:247–253
42. Sadeghi B, Rostami A, Momeni SS (2015) Facile green synthesis of silver nanoparticles using seed aqueous extract of *Pistacia atlantica* and its antibacterial activity. *Spectrochim Acta A Mol Biomol Spectrosc* 134:326–332
43. Bangale S, Ghotekar S (2019) Bio-fabrication of silver nanoparticles using *Rosa chinensis* L. extract for antibacterial activities. *Int J Nano Dimens* 10(2):217–224
44. Fleischera TC, Ameadea EPK, Sawerb IK (2003) Antimicrobial activity of the leaves and flowering tops of *Acanthospermum hispidum*. *Fitoterapia* 74:130–132
45. Harekrishna R, Anup C, Satyabrata B, Bhabani SN, Sruti Ranjan M, Ellaiah P (2010) Preliminary phytochemical investigation and anthelmintic activity of *Acanthospermum hispidum* DC. *J Pharm Sci Technol* 2:217–221
46. Artur S, Gunther MK, Thomas C, Mettenleiter B, Hanns-Joachim R, Armin S (1997) Antiviral activity of an extract from leaves of the tropical plant *Acanthospermum hispidum*. *Antiviral Res* 36:55–62
47. Sanon S, Azas N, Gasquet M, Ollivier E, Mahiou V, Barro N, Cuzin-Ouattara N, Traore AS, Esposito F, Balansard G, Timon-David P (2003) Antiplasmodial activity of alkaloid extracts from *Pavetta crassipes* (K. Schum) and *Acanthospermum hispidum* (DC), two plants used in traditional medicine in Burkina. *Faso Parasitol Res* 90:314–317
48. Deepa N, Rajendran NN (2007) Anti-tumor activity of *Acanthospermum hispidum* DC on dalton ascites lymphoma in mice. *Nat Prod Sci* 13:234–240
49. Arena ME, Cartagena E, Nadia G, Mario B, Juan CV, Alicia B (2011) In vivo and in vitro antibacterial activity of acanthospermol B, a sesquiterpene lactone isolated from *Acanthospermum hispidum*. *Phytother Res* 25:597–602
50. Abdulkarim A, Sadiq Y, Gabriel OA, Abdulkadir UZ, Ezzeldin MA (2005) Evaluation of five medicinal plants used in diarrhoea treatment in Nigeria. *J Ethnopharmacol* 101:27–30
51. Fransworth NR (1996) Biological and phytochemical screening of plants. *J Pharm Sci* 55:225–227
52. Wiegand I, Hilpert K, Hancock REW (2008) Agar and broth dilution methods to determine the minimal inhibitory concentration (MIC) of antimicrobial substances. *Nat Protoc* 3:163–175
53. Anargyros P, Astill DS, Lim IS (1990) Comparison of improved BACTEC and Lowenstein–Jensen media for culture of mycobacteria from clinical specimens. *J Clin Microbiol* 28:1288–1291
54. Riekmann KH, Campbell GH, Sax LJ, Mrema JE (1978) Drug sensitivity of *Plasmodium falciparum*: an in vitro microtechnique. *Lancet* 1:22–23
55. Singh JSB (1956) J. S. B stain: a review. *Indian J Malariol* 10:117–129
56. Patterson A (1939) The Scherrer formula for X-ray particle size determination. *Phys Rev* 56:978–982
57. Pansambal S, Deshmukh K, Savale A, Ghotekar S, Pardeshi O, Jain G, Aher Y, Pore D (2017) Phytosynthesis and biological activities of fluorescent CuO nanoparticles using *Acanthospermum hispidum* L. extract. *J Nanostruct* 7(3):165–174
58. Chakraborty AK, Gaikwad AV, Singh KB (2012) Phytopharmacological review on *Acanthospermum hispidum*. *J Appl Pharm Sci* 2(1):144–148
59. Mahajan PG, Bhopate DP, Kolekar GB, Patil SR (2015) N-methyl isatin nanoparticles as a novel probe for selective detection of Cd²⁺ ion in aqueous medium based on chelation enhanced fluorescence and application to environmental sample. *Sens Actuat B Chem* 220:864–872
60. Mahajan PG, Bhopate DP, Kamble AA, Dalavi DK, Kolekar GB, Patil SR (2015) Selective sensing of Fe²⁺ ions in aqueous solution based on fluorescence quenching of SDS capped rubrene nanoparticles: application in pharmaceutical formula. *Anal Methods* 7:7889–7898

Publisher's Note Springer Nature remains neutral with regard to jurisdictional claims in published maps and institutional affiliations.